JACS
JOURNAL OF THE AMERICAN CHEMICAL SOCIETY
Article
pubs.acs.org/JACS

Effective Panchromatic Sensitization of Electrochemical Solar Cells: Strategy and Organizational Rules for Spatial Separation of Complementary Light Harvesters on High-Area Photoelectrodes

Nak Cheon Jeong,[†,‡,*] Ho-Jin Son,[†] Chaiya Prasittichai,[†] Chang Yeon Lee,[†,§] Rebecca A. Jensen,[†] Omar K. Farha,[†] and Joseph T. Hupp[†,∥,*]

[†]Department of Chemistry, Northwestern University, 2145 Sheridan Road, Evanston, Illinois 60208, United States ,
[‡]Department of Emerging Materials Science, DGIST, Daegu 711-873, Korea,
[§]Department of Energy and Chemical Engineering, University of Incheon, Incheon 406-772, Korea, and
[∥]Argonne National Laboratory, Argonne, Illinois 60439, United States

Supporting Information

ABSTRACT: Dye-sensitized solar cells, especially those comprising molecular chromophores and inorganic titania, have shown promise as an alternative to silicon for photovoltaic light-to-electrical energy conversion. Co-sensitization (the use of two or more chromophores having complementary absorption spectra) has attracted attention as a method for harvesting photons over a broad spectral range. If implemented successfully, then cosensitization can substantially enhance photocurrent densities and light-to-electrical energy conversion efficiencies. In only a few cases, however, have significant overall improvements been obtained. In most other cases, inefficiencies arise due to unconstructive energy or charge transfer between chromophores or, as we show here, because of modulation of charge-recombination behavior. Spatial isolation of differing chromophores offers a solution. We report a new and versatile method for fabricating two-color photoanodes featuring spatially isolated chromophore types that are selectively positioned in desired zones. Exploiting this methodology, we find that photocurrent densities depend on both the relative and absolute positions of chromophores and on "local" effective electron collection lengths. One version of the two-color photoanode, based on an organic push−pull dye together with a porphyrin dye, yielded high photocurrent densities (J_{SC} = 14.6 mA cm^{-2}) and double the efficiency of randomly mixed dyes, once the dyes were optimally positioned with respect to each other. We believe that the organizational rules and fabrication strategy will prove transferrable, thereby advancing understanding of panchromatic sensitization as well as yielding higher efficiency devices.

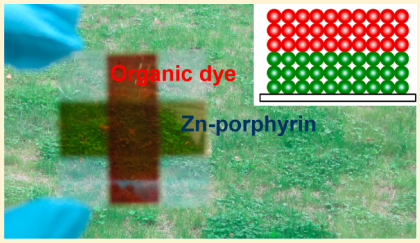

INTRODUCTION

Solar-derived electricity will likely play a substantial role in meeting the rising demand for energy in general and, more specifically, for energy from carbon-neutral sources. Dye-sensitized solar cells (DSCs), comprising chromophores, redox shuttles, and nanoporous semiconductors, have shown considerable promise as low-tech alternatives to ubiquitous, but pricey, silicon-based photovoltaics.[1−10] The most efficient DSCs display light-to-electrical energy conversion efficiencies of just over 12%.[11] Obviously, in order for DSCs to attain higher efficiencies and become genuinely competitive with silicon technology, efficiencies, and therefore, photovoltages, photocurrent densities, or both, must be increased. One approach to boosting photocurrents is to employ multiple dye types ("co-sensitization") rather than a single type, thereby broadening spectral coverage and enhancing light harvesting efficiencies (LHEs). A second general idea, applicable to increasing both open-circuit photovoltages (V_{oc}) and short-circuit photocurrent densities (J_{sc}) is to decrease the rate at which injected electrons are lost to recombination with the oxidized dye, or more commonly, the oxidized redox shuttle. To the extent the loss or recombination rate can be diminished, the effective electron collection length, L_{eff}, can be increased. L_{eff} is the average distance an injected electron travels through the photoanode before recombining;[12−15] electrons injected at distances greater than L_{eff} from the current collector will be collected with only low probability and, therefore, will seldom contribute to the photocurrent. Larger effective-collection-lengths allow thicker (i.e., higher surface area) photoelectrodes to be productively used, resulting in greater dye loading, larger LHEs, and larger photocurrents.

As described further below, we have discovered that the challenges of effective cosensitization and of L_{eff} optimization are, for many systems, closely linked. To a first approximation, one might expect L_{eff} to be insensitive to the identity of the adsorbed dye, since adsorption should have little effect upon the rate of electron transport within the photoanode. The electron collection length, however, also depends upon the rate of interception of injected electrons by the redox shut-

Received: September 3, 2012
Published: November 7, 2012

   dx.doi.org/10.1021/ja308725r | J. Am. Chem. Soc. 2012, 134, 19820−19827

tle.[12,14−16] By associating with oxidized shuttle molecules and increasing their local concentration,[17] dyes can increase interception rates by 50-fold or more, and thereby shrink L_{eff}.[18−20] Or, dyes can act as barriers to contact between the photoanode and the oxidized shuttle, thereby decreasing interception rates and increasing L_{eff}.[21,22] Thus, the collection length can be used to gauge the efficacy of recombination (and vice versa).

An ideal chromophore should yield an effective electron collection length greater than the desired thickness of the photoanode, thereby ensuring that essentially all injected electrons are captured by the current collector and contribute to J_{sc}, the short-circuit current density. An ideal dye also should absorb strongly throughout the visible spectrum and extend a few tenths of an eV into the near-infrared region. Difficulty in developing a single dye capable of panchromatic sensitization has prompted several researchers to explore cosensitization of photoelectrodes using mixtures of complementarily absorbing dyes;[11,23−32] indeed, this strategy was employed to push the efficiencies of well-designed DSCs from ca. 11.5%[33] (single chromophore) to the current record of 12.3%.[11] More typical of studies of *mixed cosensitization* are the results of McGehee and co-workers, who found that DSCs featuring mixed chromophores under-performed those employing a single-component chromophore, despite broader spectral coverage for the former. From elegant mechanistic studies, the culprit was shown to be unproductive charge transfer between chromophores of differing composition.[9,32]

A potentially attractive alternative would be cosensitization with *spatially separated* (and, therefore, noninterfering) chromophore types. To date, two approaches have been discussed—one mimicking column chromatography and the other entailing transferring TiO_2 films with friction.[34−36] While both are intriguing, both present limitations (e.g., substantial residual overlap of nominally single-dye-type zones, inability to reverse the positioning of pairs of dye types within a porous photoelectrode, and/or spatially intermittent electrical contact between component layers of a photoelectrode). More problematic is the current lack of guidelines (apart from spectral complementarity) for choosing pairs of chromophores and for determining how they can be best organized or positioned with respect to each other. In this report, we present a new method for fabricating photoanodes featuring spatially separated light-harvesting zones and demonstrate how effective-electron-collection-lengths (L_{eff} values) and the positions of the chromophores significantly affect photocurrent generation via cosensitization. This approach should aid researchers by helping them to identify dye combinations likely to give high efficiencies in both mixed and spatially separated cosensitization configurations. Using the latter, we have obtained photoelectrodes that yield high photocurrent densities (up to 14.6 mA cm^{-2}) using comparatively simple pairs of visible-region chromophores.

RESULTS AND DISCUSSION

Effective Electron Collection Lengths of Dye-Coated Electrodes. O'Regan and co-workers have shown that chromophore-specific L_{eff} values for photoelectrodes can be obtained by measuring and evaluating the wavelength-dependent ratio of photocurrents ($r_{j(CE/PE)}$) generated by illuminating DSCs from the counter-electrode (CE) side versus photoelectrode (PE) side (Figure 1b).[12,13] Their analysis derives from the fact that the population of photoinjected electrons

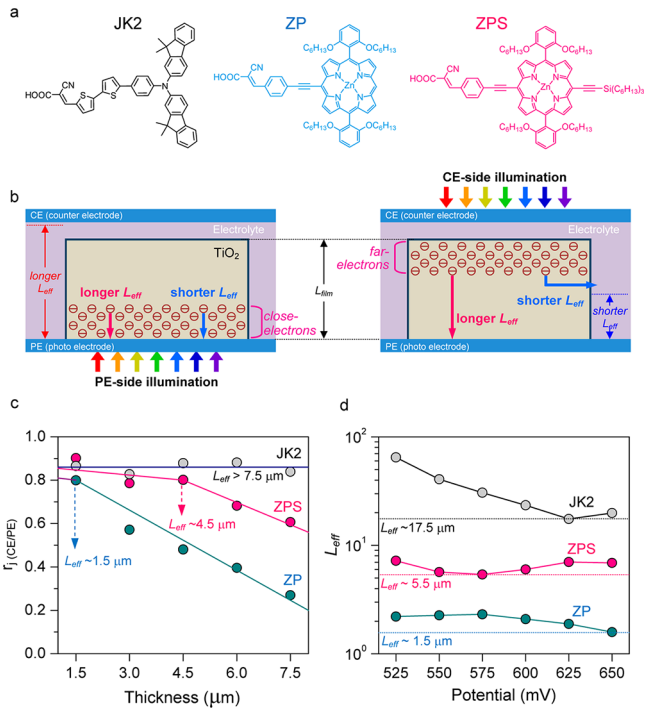

Figure 1. (a) Structures of JK2, ZP, and ZPS. (b) Schematics for the population of electrons generated by PE- and CE-side illuminations. (c) Ratios of photocurrent density generated by PE-side and CE-side illumination as a function of TiO_2 film thicknesses in photoanodes coated with JK2, ZP, or ZPS (see Supporting Information Section S3). Illumination done at 560, 630, or 650 nm. (d) L_{eff} values with JK2, ZP, and ZPS measured by EIS as a function of applied potential.

through the depth of a photoanode is nonuniform. More photons are absorbed in the regions nearer the light source and, therefore, more electrons are injected, resulting (at least at short circuit) in a roughly exponential distribution of injected electrons through the depth of the electrode. In cells with transparent counter-electrodes, illumination from either direction is possible. Regardless of the direction of illumination, we will denote the electrons injected close to the FTO current collector as *close-electrons*, and those injected distant from the current collector as *far-electrons* (see Figure 1b).

If, for a particular photoanode/chromophore combination, L_{eff} is less than the physical thickness of a porous photoelectrode film (L_{film}), then most far-electrons will be lost to recombination during their trip through the TiO_2 network, while most close-electrons will be collected and will contribute to the photocurrent (Figure 1b). The ratio, $r_{j(CE/PE)}$, will be considerably less than unity. However, if L_{eff} exceeds the physical thickness of the film, most electrons will be captured regardless of the direction of illumination, and therefore, $r_{j(CE/PE)}$ will be close to unity.

With this in mind, we measured values of $r_{j(CE/PE)}$ for electrodes sensitized by a representative push−pull dye, JK2, or by either of two zinc porphyrin dyes, ZP and ZPS. (See Figure 1a and Supporting Information Section S1 for syntheses. Notably, the absorption spectra for both porphyrin dyes are complementary to the push−pull dye.) By measuring values as a function of photoelectrode film thickness, we expect to be able to obtain model-independent estimates of L_{eff}. Briefly, the effective electron collection length would correspond to a critical photoelectrode thickness beyond which $r_{j(CE/PE)}$ drops rapidly. Using a homemade paste[37] as the TiO_2 source, we

dx.doi.org/10.1021/ja308725r | J. Am. Chem. Soc. 2012, 134, 19820−19827

Table 1. Parameters of Photovoltaic Performance Measured at Simulated (AM 1.5) One Sun[a]

types	samples ($[\text{bottom}\backslash\text{top}]_{T\ (\mu m)}$)	J_{SC} (mA cm^{-2})	V_{OC} (V)	*FF*	η (%)
separated cosensitization	$[ZP]_{4.5}$	5.94 (4.6)	0.60	0.70	2.49
	$[-\backslash JK2]_{4.5\backslash 4.5}$	8.85 (8.2)	0.69	0.73	4.46
	$[ZP\backslash JK2]_{4.5\backslash 4.5}$	7.01 (6.2)	0.62	0.72	3.13
	$[JK2]_{4.5}$	9.96 (9.6)	0.71	0.67	4.74
	$[-\backslash ZP]_{4.5\backslash 4.5}$	5.44 (4.3)	0.59	0.69	2.21
	$[JK2\backslash ZP]_{4.5\backslash 4.5}$	11.36 (10.3)	0.65	0.71	5.24
	$[ZPS]_{4.5}$	9.69 (9.5)	0.64	0.67	4.16
	$[-\backslash JK2]_{4.5\backslash 4.5}$	8.85 (8.3)	0.69	0.73	4.46
	$[ZPS\backslash JK2]_{4.5\backslash 4.5}$	12.47 (11.6)	0.67	0.72	6.02
	$[JK2]_{4.5}$	9.96 (9.6)	0.71	0.67	4.74
	$[-\backslash ZPS]_{4.5\backslash 4.5}$	8.42 (8.0)	0.64	0.69	3.72
	$[JK2\backslash ZPS]_{4.5\backslash 4.5}$	13.67 (13.1)	0.67	0.70	6.41
	$[JK2\backslash ZPS\backslash SL]_{4.5\backslash 4.5}$	14.63 (14.1)	0.68	0.69	6.86
mixed cosensitization	$[JK2+ZP]_{1.5}$	7.04 (6.8)	0.66	0.70	3.25
	$[JK2+ZP]_{3.0}$	8.53 (8.3)	0.63	0.68	3.65
	$[JK2+ZP]_{4.5}$	8.22 (7.4)	0.61	0.70	3.51
	$[JK2+ZP]_{6.0}$	6.88 (6.2)	0.59	0.70	2.84
	$[JK2+ZP]_{7.5}$	6.15 (5.7)	0.58	0.72	2.57
	$[JK2+ZPS]_{1.5}$	7.97 (7.5)	0.69	0.68	3.74
	$[JK2+ZPS]_{3.0}$	9.04 (8.7)	0.67	0.67	4.06
	$[JK2+ZPS]_{4.5}$	9.96 (9.7)	0.64	0.67	4.27
	$[JK2+ZPS]_{6.0}$	9.66 (9.1)	0.63	0.65	3.96
	$[JK2+ZPS]_{7.5}$	9.23 (8.6)	0.61	0.64	3.60

[a]The numbers in parentheses are estimated values of J_{SC} obtained by integrating IPCEs.

varied the electrode thickness from 1.5 to 7.5 μm, in 1.5 μm increments, and measured photocurrent ratios at 560, 630, and 650 nm for JK2, ZP, and ZPS, respectively (see Figure 1c and Supporting Information Section S3). With the dye, JK2, values of $r_{j(CE/PE)}$ are constant (ca. 0.85), indicating that L_{eff} equals or exceeds 7.5 μm. (The deviation of the ratio from unity likely is due to fixed light losses assignable to less than complete transparency for the counter-electrode.) With ZP as the chromophore, $r_{j(CE/PE)}$ is large (~0.8) only with 1.5 μm electrodes, decreasing drastically as the film thickness is made greater. From this behavior, L_{eff} is ~1.5 μm. With ZPS as the chromophore, $r_{j(CE/PE)}$ values are large (>0.8) for electrodes of thickness 1.5, 3.0, or 4.5 μm, but decrease substantially as the thickness is made greater. From these experiments we conclude that L_{eff} is ~4.5 μm. The substantial difference in L_{eff} for ZPS- versus ZP-coated electrodes is remarkable in view of the structural similarities of the chromophores, but not without precedent.[18] We tentatively ascribe the difference (which is minimal with other redox shuttles) to a difference in the strength of dye/tri-iodide association.

The chromophore-dependent values of L_{eff} are in good agreement with results obtained via electrochemical impedance spectroscopy (EIS). (For details, see Figure 1d and Supporting Information Section S3). Values for the charge-collection length vary somewhat with potential, typically decreasing at higher potentials. The smallest EIS-derived collection lengths we observed were 17.5, 1.5, and 5.5 μm, for JK2, ZP, and ZPS, respectively. (Exact agreement between the two types of L_{eff} measurements is not expected, since the EIS measurements will miss any contributions due to charge recombination with the dye (as opposed to the shuttle) and since the local photoelectrode potential as a function of distance from the current collector will vary in different ways for photochemical versus electrochemical (i.e., EIS) injection of electrons. Nevertheless, the observed close agreement between the two types of measurements provides excellent supporting evidence that L_{eff} indeed does depend strongly upon the chemical identity of the chromophore.)

***Mixed Cosensitization* with JK2 and ZP ([JK2 + ZP]).** We next prepared cells containing 4.5 μm-thick TiO_2 films that had been dye-loaded from a 1:1 solution mixture of JK2 and ZP ($[JK2 + ZP]_{4.5}$). For comparison, DSCs containing single-chromophore films of JK2 ($[JK2]_{4.5}$) or ZP ($[ZP]_{4.5}$) were also constructed. Cells containing $[JK2 + ZP]_{4.5}$ photoelectrodes yielded much smaller photocurrents than either of the cells sensitized with single chromophores, despite superior LHEs with mixed cosensitization (see Supporting Information Section S6 and Table 1). The incident-photon-to-current conversion efficiency (IPCE) spectrum of a DSC containing $[JK2 + ZP]_{4.5}$ showed an increase of efficiency relative to $[JK2]_{4.5}$, in the 600−700 nm range, owing to the presence of ZP, a good absorber of red photons. Over the 400 to 600 nm range, however, the efficiency of the DSC containing $[JK2 + ZP]_{4.5}$ was less than seen with DSC based on $[JK2]_{4.5}$. We considered two explanations for the inferior performance of the mixed cosensitizers: (i) lower loading and, therefore, diminished light harvesting by JK2 (due to competitive adsorption of ZP on the porous electrode), and (ii) acceleration, by ZP, of the rate of electron interception by tri-iodide. The first possibility was tested by preparing a DSC containing a 7.5-μm thick photoelectrode, thereby increasing the absolute quantity of each dye present. Remarkably, photocurrent densities with $[JK2 + ZP]_{7.5}$ were even smaller than with $[JK2 + ZP]_{4.5}$—leaving the second possibility (evaluated further, below) as the default explanation.

To quantify L_{eff}, we measured $r_{j(CE/PE)}$ values as a function of film thickness for electrodes cosensitized by JK2 and ZP. A drastic drop in $r_{j(CE/PE)}$ beyond a thickness of 3.0 μm, establishes $L_{eff} \approx 3.0$ μm (see Supporting Information (SI) Section S6, Figure S9).

dx.doi.org/10.1021/ja308725r | J. Am. Chem. Soc. 2012, 134, 19820−19827

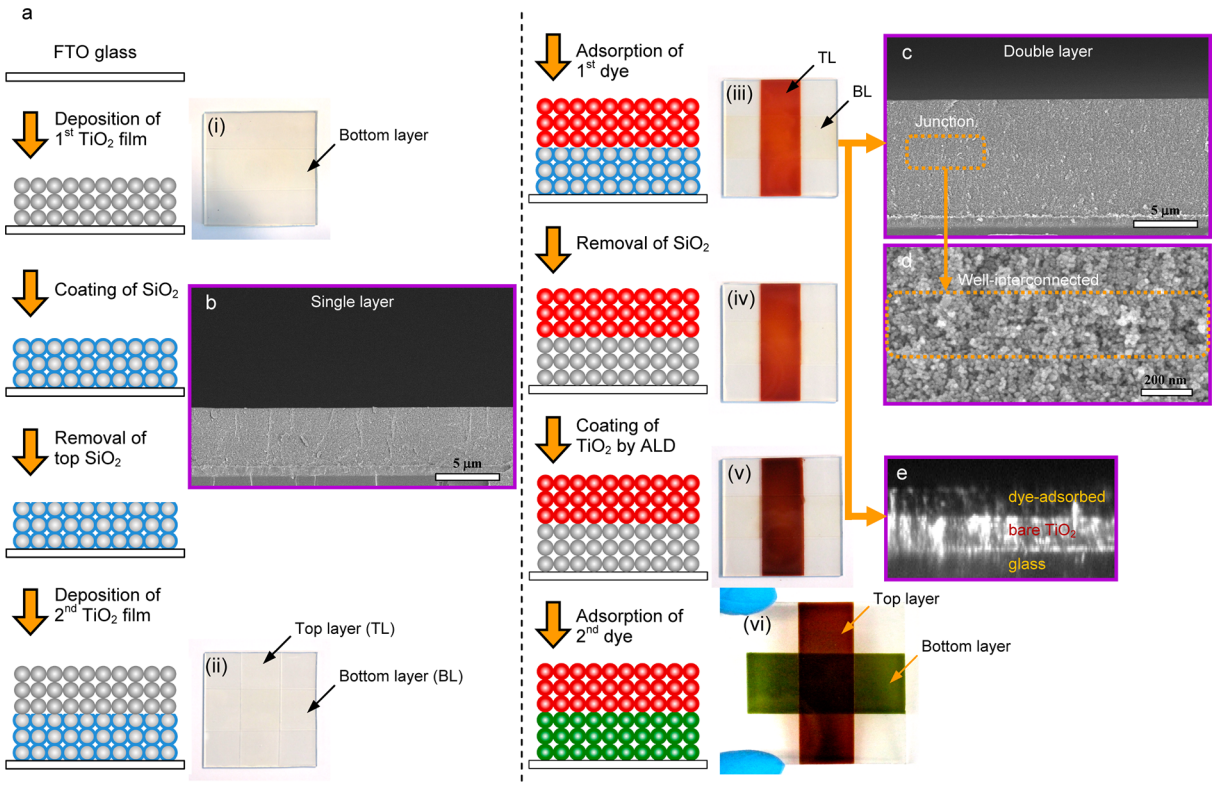

Figure 2. (a) Schematic procedure for the fabrication of two-color-photoanodes. (b, c) Scanning electron microscope (SEM) images of single and double layered, nanoporous TiO_2 films as indicated. (d) Magnified SEM image at the junction area between top and bottom TiO_2 layers. (e) Cross-sectional optical microscope image after the first chromophore adsorbed. (i)−(vi), Photographs of TiO_2 films at each step.

Fabrication of Photoanodes for *Spatially Separated Cosensitization*. In light of the above results and preliminary interpretation, we reasoned that better-performing cells might be obtained by using electrodes featuring distinct, non-overlapping zones of only JK2 or only a porphyrinic chromophore. To obtain such structures, we developed a TiO_2 passivation-restoration strategy that takes advantage of the fact that dyes possessing carboxylate anchors do not adsorb on annealed SiO_2 surfaces. Passivation and restoration, respectively, were executed by coating TiO_2 with SiO_2 and by removing the SiO_2 with dilute aq. HF. (***Caution:*** *HF is easily absorbed through skin and, when absorbed, can be highly toxic. For safe handling, appropriate protective equipment, including silver-lined gloves, must be used, and contingencies for spills must be in place.*) The fabrication protocol is illustrated in Figure 2. A transparent 4.5 μm-thick TiO_2 film was deposited on electrically conductive glass (fluorine-doped tin-oxide coated glass). The film was then coated with SiO_2. Silica residing on the top of the TiO_2 film was selectively removed by briefly brushing the film with a sample of cotton that had been wetted with dilute HF. A second TiO_2 layer was then deposited atop the first (for details, see SI Section S4). Scanning electron microscopy (SEM) showed that TiO_2 nanoparticles in the junction area between the top and bottom layers are well interconnected (see Figure 2c,d). (We note that removal of SiO_2 from the top of the first layer is a crucial step. If omitted, then the nanonetwork around the junction is poorly interconnected physically as well as electronically. The consequences are blockage of electron transport across the junction and catastrophic loss of photocurrent from the upper layer of the photoelectrode (see SI Section S8). As shown by the photograph in Figure 2(iii), the first chromophore is selectively adsorbed on the upper (unprotected) TiO_2 layer, with almost none adsorbing on the lower, SiO_2-passivated layer. These observations were confirmed via cross-sectional optical microscopy (Figure 2e). Next, the SiO_2 coating was completely removed with dilute HF solution, and the porous film was conformally coated with an ultrathin layer of TiO_2 (~7 Å) via atomic layer deposition (ALD), in order to reinforce the anchoring of dye molecules to the film's upper layer (SI Section S9). Finally, the assembly was exposed to a second dye. (In the absence of the ALD step, we found that the second dye could sometimes displace the first dye and coat the entire electrode.) A photograph in Figure 2(vi), taken after the second dye was applied, shows a cross with two colors. In this case, the vertical bar (dark red) is the top layer in the overlapping region and is selectively coated with JK2. The horizontal bar (green) is the bottom layer in the overlapping region and is selectively coated with ZP. The square center region is coated, in spatially selective fashion, with two chromophores and is dark brown (i.e., nearly panchromatic).

***Spatially Separated Cosensitization* with JK2 and ZP ([JK2\ZP] and [ZP\JK2]).** Photoelectrodes comprising a ZP lower layer and a JK2 upper layer (designated [ZP\JK2]) were fabricated (Figure 3a). The thickness of each layer was 4.5 μm. Also constructed were DSCs with electrodes featuring a ZP-coated lower layer and an empty upper layer ([ZP]) or, an empty lower layer and a JK2-coated upper layer ([−\JK2]). One might have expected that adding complementary light harvesters to [−\JK2] to form [ZP\JK2] would increase the overall photocurrent density (see Section S10 of the SI for LHE comparisons). Instead, we find that the current density is significantly reduced (Figure 3b and Table 1).

dx.doi.org/10.1021/ja308725r | J. Am. Chem. Soc. 2012, 134, 19820−19827

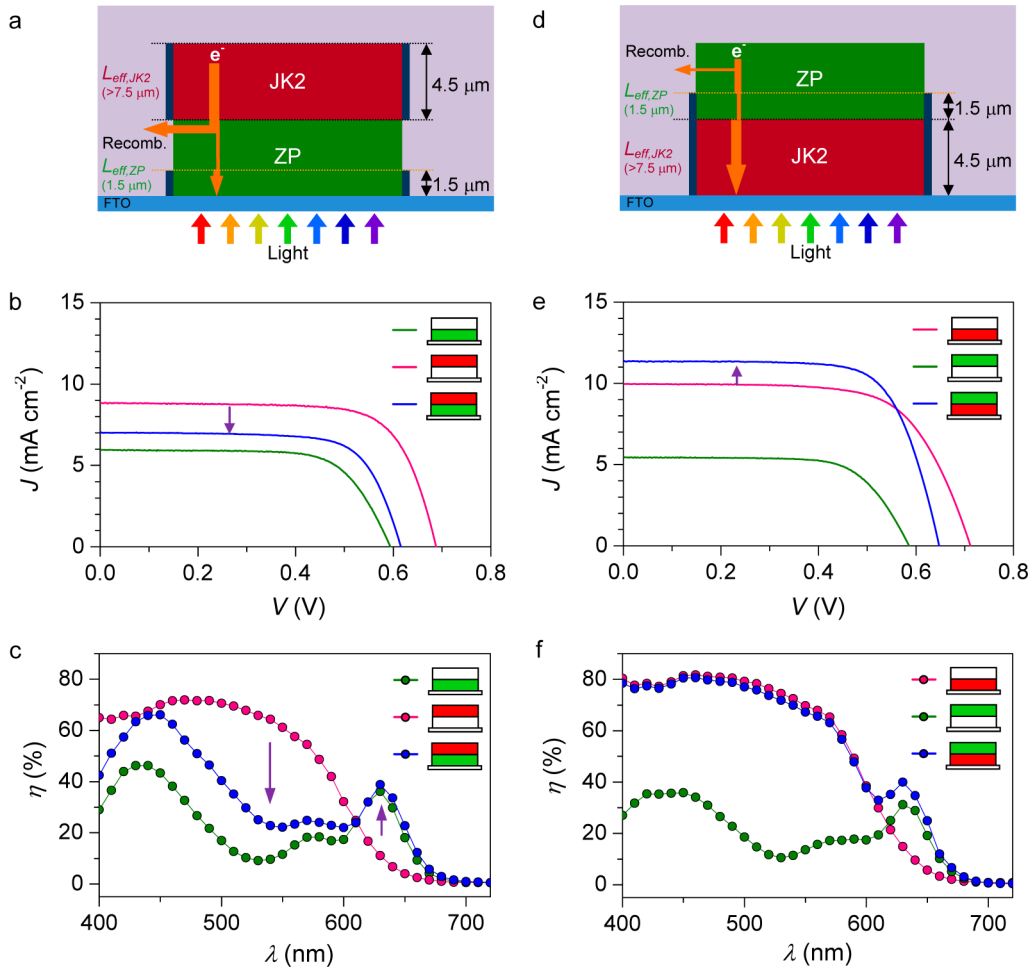

Figure 3. (a) and (d) Schematic illustration for the configuration and electron collection of a two-color photoanode with JK2 and ZP chromophores. (b) JV curves and (c) IPCE spectra of [ZP\–], [–\JK2], and [ZP\JK2] as indicated. (e) JV curves and (f) IPCE spectra of [JK2\–], [–\ZP], and [JK2\ZP] as indicated.

Figure 3c shows IPCE plots for all three types of photoelectrodes. Notably, photocurrent output from [ZP\JK2] is higher than that of [ZP] over the entire spectral range, but lower than that of [–\JK2] in the range from 450 to 600 nm. These observations indicate that electrons generated by ZP within the above-determined L_{eff} (1.5 μm) are successfully collected. However, regardless of where they originate, injected electrons are largely lost when attempting to pass through a ZP-coated region whose thickness exceeds this L_{eff} value (see scheme in Figure 3a).

In contrast to [ZP\JK2], photoelectrodes having the chromophore locations reversed (i.e., [JK2\ZP], see Figure 3d) yielded overall photocurrent densities that exceeded those from either type of single-dye photoelectrode, i.e., [JK2] or [–\ZP] (see Figure 3e and Table 1). The IPCE spectrum in Figure 3f for [JK2\ZP] shows that photocurrents in the 400 to 600 nm region are dominated by JK2, while in the 600 to 700 nm region they are due mainly to ZP. These observations indicate that electrons generated in either the JK2 or ZP layer can successfully navigate the JK2 layer and contribute to the photocurrents. Note that the characteristic electron-collection length for electrodes (or portions of electrodes) coated with JK2 (ca. 17 μm) substantially exceeds the physical thickness of the JK2 zone (4.5 μm). In contrast, the characteristic electron-collection length for ZP-coated electrodes or zones is small relative to the physical thickness of the ZP layers examined here (i.e., 1.5 μm versus 4.5 μm). Consequently, light harvesting by ZP contributes only marginally to the photocurrent obtained from [JK2\ZP] (see Figure 3 and Table 1).

***Mixed Cosensitization* with JK2 and ZPS ([JK2 + ZPS]).** The above result emphasizes that, in cosensitization, the magnitude of L_{eff} and the position of the chromophore engendering the shorter collection length govern the overall photocurrent collection ability of the system. We reasoned that cosensitization would be most effective, and photocurrent densities largest, in DSCs featuring pairs of chromophores, both of which engender comparatively large values for L_{eff}. Therefore, we prepared cells containing photoelectrodes of coated with mixtures JK2 and ZPS ($[JK2 + ZPS]_{4.5}$), as well as controls featuring only one chromophore, i.e. $[JK2]_{4.5}$ or ZPS cell $[ZPS]_{4.5}$. Disappointingly, the overall photocurrent output from $[JK2 + ZPS]_{4.5}$ was nearly identical to that from $[ZPS]_{4.5}$ or $[JK2]_{4.5}$ (see SI Section S7 and Table 1). The IPCE spectrum of $[JK2 + ZPS]_{4.5}$ in the 600 to 700 nm contains contributions clearly attributable to ZPS. Furthermore, the porphyrin-derived contributions in mixed-chromophore DSCs are greater from ZPS than from ZP (see above). The observed gains in the red region with ZPS are offset by efficiency decreases in the blue part of the spectrum. We also examined mixed sensitization of photoelectrodes of nearly double the

dx.doi.org/10.1021/ja308725r | J. Am. Chem. Soc. 2012, 134, 19820–19827

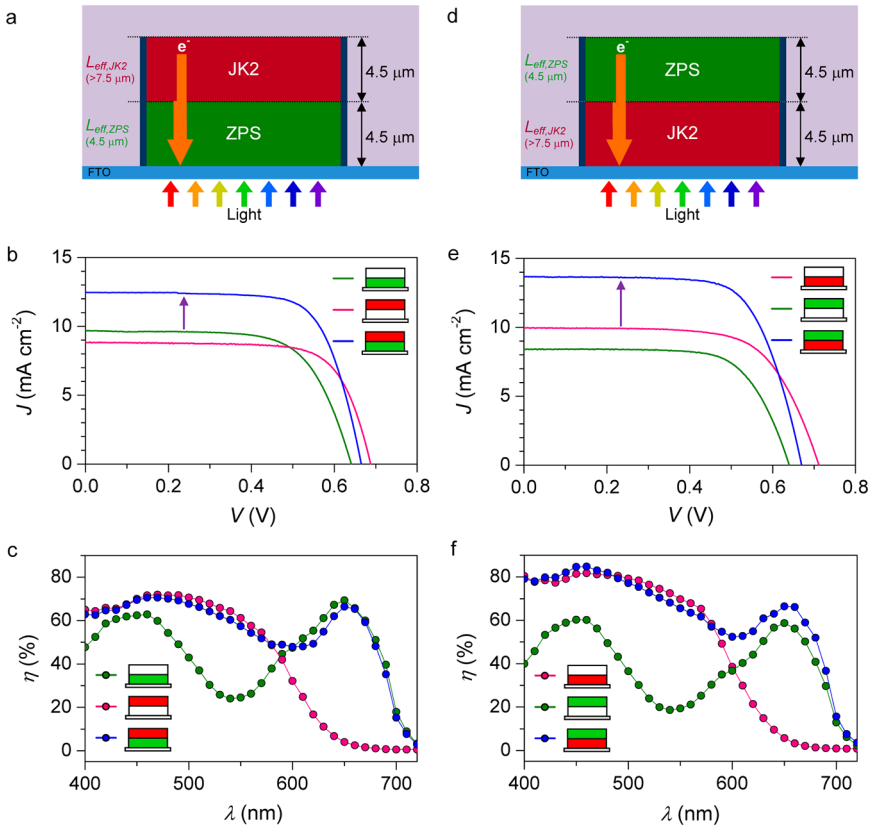

Figure 4. (a) and (d) Schematic illustration for the configuration and electron collection of a two-color photoanode with JK2 and ZPS. (b) JV curves and (c) IPCE spectra of [ZPS\−], [−\JK2], and [ZPS\JK2] as indicated. (e) JV curves and (f) IPCE spectra of [JK2\−], [−\ZPS], and [JK2\ZPS] as indicated.

initial thickness, i.e., 7.5 versus 4.5 μm, as well as less thick structures (SI Section S7). J_{sc} maximized at 4.5 μm, while $r_{j(CE/PE)}$ was constant through 4.5 μm, but smaller for greater thicknesses. These observations are consistent with the L_{eff} value engendered by ZPS alone (4.5 μm) and illustrate that the dye associated with less effective charge collection defines L_{eff} for mixed chromophore coatings.

***Spatially Separated Cosensitization* with JK2 and ZPS ([JK2\ZPS] and [ZPS\JK2]).** Convinced that the above findings would justify the spatial separation of chromophores, we prepared a photoelectrode featuring a ZPS-coated lower layer and a JK2-coated upper layer (designated [ZPS\JK2]) (Figure 4a). The thickness of each layer was 4.5 μm. For comparison, electrodes featuring a ZPS-coated lower layer and an empty upper layer ([ZPS]) or, an empty lower layer and a JK2-coated upper layer ([−\JK2]) were also fabricated. In contrast to DSCs based on [ZP\JK2], the photocurrent density of the [ZPS\JK2] based cell was substantially greater than found with DSCs based on either of the half-filled, single-dye photoelectrode control cells (see Figure 4b and Table 1). The IPCE spectrum with [ZPS\JK2] reveals that photocurrent in the range from 600 to 700 nm is mainly generated via photoexcitation of ZPS (Figure 4c), while in the 400 to 600 nm range both dyes significantly contribute. Dual sensitization in the 400 to 600 nm range occurs because (a) ZPS first harvests a fraction of the light, with JK2 harvesting most of the transmitted remnant, and (b) injected electrons are collected from throughout the photoelectrode (see SI Section S10). The similarity of the IPCE spectra for [ZPS\JK2] and [−\JK2] in the 400 to 570 nm range implies that LHEs (in this range) are already close to unity for both ZPS and JK2, and that injected electrons are transported to the current collector with minimal loss due to interception by tri-iodide.

When we reversed the siting of ZPS and JK2 (see Figure 4d), the photocurrent density was further enhanced (Figure 4e and Table 1). IPCE measurements show that photocurrent generation in the 400 to 600 nm region is dominated by contributions from JK2, while in the 600 to 700 nm region it is dominated by ZPS. These results indicate that most of the electrons injected by JK2 and ZPS are subsequently collected and clearly are consistent with the comparatively large L_{eff} values measured for JK2 and ZPS (>7.5 and 4.5 μm, respectively) (Figure 4d). Thus, the photocurrent density of the [JK2\ZPS] photoanode exceeds by 3.7 and 5.2 mA cm^{-2}, respectively, photocurrent densities generated by [JK2] and [−\ZPS] (see Table 1).

Modulation of Lower Layer Thickness with [ZP\JK2] and [ZPS\JK2]. In order to corroborate our findings and conclusions, we additionally examined photoelectrodes having a lower-layer thickness of 1.5, 3.0, 4.5, 6.0, or 7.5 μm, keeping the thickness of the upper layer at 4.5 μm. For [ZP\JK2] structures, both J_{sc} and V_{oc} were highest at 1.5 μm, despite the ability of thicker structures to capture more light (see Figure 5 and SI Section S11). In contrast, the photocurrent density with [ZPS\JK2] was maximized at 4.5 μm and V_{oc} remaining constant up to this thickness. These thicknesses agree well with the corresponding L_{eff} values for of ZP- and ZPS-coated electrodes.

Effects of Scattering-Layer Addition. With the aim of attaining yet higher efficiency, we added a TiO_2 scattering layer to an optimized version of [JK2\ZPS], yielding [JK2\ZPS\SL].

dx.doi.org/10.1021/ja308725r | J. Am. Chem. Soc. 2012, 134, 19820−19827

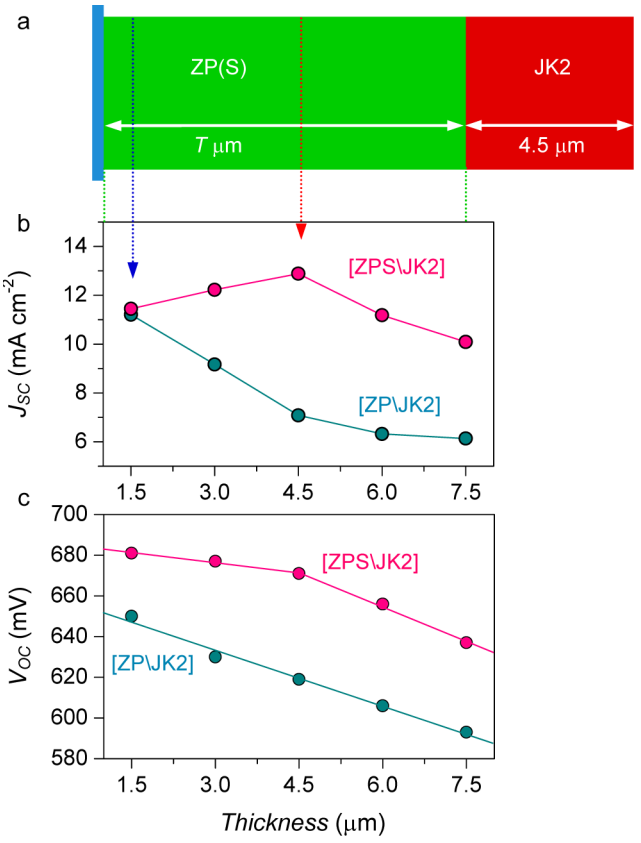

Figure 5. Correlation between electron collection length and actual film thickness of lower layer. (a) Schematic illustration for the configuration of [ZP\JK2] or [ZPS\JK2], and (b) plot of short-circuit current and (c) open-circuit voltage changes versus lower-layer thickness.

The optimized thicknesses of lower (JK2) and upper (ZPS) layers were 4.5 and 3.0 μm, respectively. Addition of the scattering layer boosted photocurrent densities of cells by 1.0 mA cm^{-2} and energy conversion efficiencies by an absolute percentage of 0.45 (to 6.9%), primarily by improving light harvesting between 600 and 700 nm (Figure 6 and Table 1).

CONCLUSIONS

We have developed a new method to fabricate photoanodes for *spatially separated cosensitization*, in which complementary chromophores are sited in predetermined regions. For the examples examined, we find that confining different types of light harvesters to different zones can increase efficiencies by up to 104%, relative to mixed cosensitization. We have also demonstrated that the ability to generate photocurrent is highly dependent on not only the effective electron collection length engendered by each chromophore, but also the positions of the chromophores with respect to each other. In contrast, the efficiency of current collection does not depend on the chromophoric origin of the electrons being collected. While the initially tested chromophores were chosen primarily for their usefulness in enabling hypotheses to be evaluated and assembly principles identified, rather than for their ability to yield highly efficient dye cells, a DSC featuring *spatially separated cosensitization* (with JK2 and ZPS) yielded comparatively high values for both the photocurrent density (14.6 mA cm^{-2}) and overall energy conversion efficiency (~7%). We anticipate that both the experimental approach and the resulting guidelines for organizing light-harvesters will prove transferrable/adaptable to other, more highly chromophoric systems—as well as other redox shuttles—thereby facilitating the design and construction of superior DSCs.

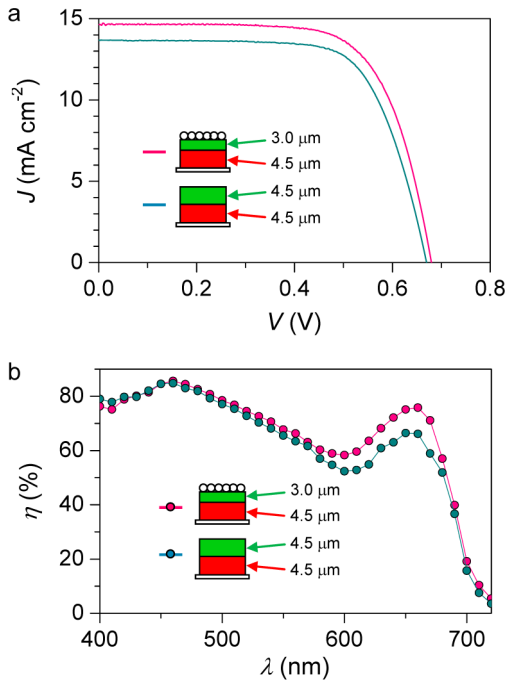

Figure 6. JV (a) and IPCE (b) curves of [JK2\ZPS] with and without scattering layer as indicated.

ASSOCIATED CONTENT

Supporting Information

Experimental details, synthetic procedures for chromophores, absorption spectra, LHE data, and supplemental JV and IPCE curves. This material is available free of charge via the Internet at http://pubs.acs.org.

AUTHOR INFORMATION

Corresponding Author

nc@dgist.ac.kr; j-hupp@northwestern.edu

Author Contributions

The manuscript was written through contributions of all authors. All authors have given approval to the final version of the manuscript.

Notes

The authors declare no competing financial interest.

ACKNOWLEDGMENTS

We gratefully acknowledge support from the U.S. Department of Energy through grants from BES (DE-FG02-87ER13808) and EERE (DE-FG36-08GO18137) for studies of molecular light harvesters and structured photoelectrodes, respectively.

REFERENCES

(1) Oregan, B.; Gratzel, M. *Nature* **1991**, *353*, 737−740.
(2) Gratzel, M. *Nature* **2001**, *414*, 338−344.
(3) Hagfeldt, A.; Gratzel, M. *Acc. Chem. Res.* **2000**, *33*, 269−277.
(4) Hamann, T. W.; Jensen, R. A.; Martinson, A. B. F.; Van Ryswyk, H.; Hupp, J. T. *Energy Environ. Sci.* **2008**, *1*, 66−78.
(5) Martinson, A. B. F.; Hamann, T. W.; Pellin, M. J.; Hupp, J. T. *Chem.-A Eur. J.* **2008**, *14*, 4458−4467.

(6) Snaith, H. J. *Adv. Funct. Mater.* **2010**, *20*, 13−19.
(7) Meyer, G. J. *ACS Nano* **2010**, *4*, 4337−4343.
(8) Kalyanasundaram, K. *Dye-Sensitized Solar Cell*, 1st ed.; EPFL Press: Lausanne, 2010.
(9) Hardin, B. E.; Snaith, H. J.; McGehee, M. D. *Nat. Photonics* **2012**, *6*, 162−169.
(10) Listorti, A.; O'Regan, B.; Durrant, J. R. *Chem. Mater.* **2011**, *23*, 3381−3399.
(11) Yella, A.; Lee, H.-W.; Tsao, H. N.; Yi, C.; Chandiran, A. K.; Nazeeruddin, M. K.; Diau, E. W.-G.; Yeh, C.-Y.; Zakeeruddin, S. M.; Grätzel, M. *Science* **2011**, *334*, 629−634.
(12) Barnes, P. R. F.; Liu, L. X.; Li, X. E.; Anderson, A. Y.; Kisserwan, H.; Ghaddar, T. H.; Durrant, J. R.; O'Regan, B. C. *Nano Lett.* **2009**, *9*, 3532−3538.
(13) Barnes, P. R. F.; Anderson, A. Y.; Koops, S. E.; Durrant, J. R.; O'Regan, B. C. *J. Phys. Chem. C* **2009**, *113*, 1126−1136.
(14) Bisquert, J.; Fabregat-Santiago, F.; Mora-Sero, I.; Garcia-Belmonte, G.; Gimenez, S. *J. Phys. Chem. C* **2009**, *113*, 17278−17290.
(15) Peter, L. M. *J. Phys. Chem. C* **2007**, *111*, 6601−6612.
(16) Barnes, P. R. F.; Anderson, A. Y.; Durrant, J. R.; O'Regan, B. C. *Phys. Chem. Chem. Phys.* **2011**, *13*, 5798−5816.
(17) Pastore, M.; Mosconi, E.; De Angelis, F. *J. Phys. Chem. C* **2012**, *116*, 5965−5973.
(18) O'Regan, B. C.; Walley, K.; Juozapavicius, M.; Anderson, A.; Matar, F.; Ghaddar, T.; Zakeeruddin, S. M.; Klein, C.; Durrant, J. R. *J. Am. Chem. Soc.* **2009**, *131*, 3541−3548.
(19) Splan, K. E.; Massari, A. M.; Hupp, J. T. *J. Phys. Chem. B* **2004**, *108*, 4111−4115.
(20) Marinado, T.; Nonomura, K.; Nissfolk, J.; Karlsson, M. K.; Hagberg, D. P.; Sun, L.; Mori, S.; Hagfeldt, A. *Langmuir* **2009**, *26*, 2592−2598.
(21) Tian, H. N.; Yu, Z.; Hagfeldt, A.; Kloo, L.; Sun, L. *J. Am. Chem. Soc.* **2011**, *133*, 9413−9422.
(22) Dunn, H. K.; Westin, P. O.; Staff, D. R.; Peter, L. M.; Waker, A. B.; Boschloo, G.; Hagfeldt, A. *J. Phys. Chem. C* **2011**, *115*, 13932−13937.
(23) Clifford, J. N.; Palomares, E.; Nazeeruddin, K.; Thampi, R.; Gratzel, M.; Durrant, J. R. *J. Am. Chem. Soc.* **2004**, *126*, 5670−5671.
(24) Fan, S. Q.; Kim, C.; Fang, B.; Liao, K. X.; Yang, G. J.; Li, C. J.; Kim, J. J.; Ko, J. *J. Phys. Chem. C* **2011**, *115*, 7747−7754.
(25) Kuang, D.; Walter, P.; Nuesch, F.; Kim, S.; Ko, J.; Comte, P.; Zakeeruddin, S. M.; Nazeeruddin, M. K.; Gratzel, M. *Langmuir* **2007**, *23*, 10906−10909.
(26) Yum, J. H.; Jang, S. R.; Walter, P.; Geiger, T.; Nuesch, F.; Kim, S.; Ko, J.; Gratzel, M.; Nazeeruddin, M. K. *Chem. Commun.* **2007**, *43*, 4680−4682.
(27) Choi, H.; Kim, S.; Kang, S. O.; Ko, J. J.; Kang, M. S.; Clifford, J. N.; Forneli, A.; Palomares, E.; Nazeeruddin, M. K.; Gratzel, M. *Angew. Chem., Int. Ed.* **2008**, *47*, 8259−8263.
(28) Siegers, C.; Hohl-Ebinger, J.; Zimmerrnann, B.; Wurfel, U.; Mulhaupt, R.; Hinsch, A.; Haag, R. *ChemPhysChem* **2007**, *8*, 1548−1556.
(29) Siegers, C.; Wurfel, U.; Zistler, M.; Gores, H.; Hohl-Ebinger, J.; Hinsch, A.; Haag, R. *ChemPhysChem* **2008**, *9*, 793−798.
(30) Hardin, B. E.; Hoke, E. T.; Armstrong, P. B.; Yum, J. H.; Comte, P.; Torres, T.; Frechet, J. M. J.; Nazeeruddin, M. K.; Gratzel, M.; McGehee, M. D. *Nat. Photonics* **2009**, *3*, 406−411.
(31) Hardin, B. E.; Yum, J. H.; Hoke, E. T.; Jun, Y. C.; Pechy, P.; Torres, T.; Brongersma, M. L.; Nazeeruddin, M. K.; Gratzel, M.; McGehee, M. D. *Nano Lett.* **2010**, *10*, 3077−3083.
(32) Hardin, B. E.; Sellinger, A.; Moehl, T.; Humphry-Baker, R.; Moser, J. E.; Wang, P.; Zakeeruddin, S. M.; Gratzel, M.; McGehee, M. D. *J. Am. Chem. Soc.* **2011**, *133*, 10662−10667.
(33) Nazeeruddin, M. K.; De Angelis, F.; Fantacci, S.; Selloni, A.; Viscardi, G.; Liska, P.; Ito, S.; Bessho, T.; Gratzel, M. *J. Am. Chem. Soc.* **2005**, *127*, 16835−16847.
(34) Lee, K.; Park, S. W.; Ko, M. J.; Kim, K.; Park, N. G. *Nat. Mater.* **2009**, *8*, 665−671.
(35) Huang, F.; Chen, D.; Cao, L.; Caruso, R. A.; Cheng, Y.-B. *Energy Environ. Sci.* **2011**, *4*, 2803−2806.
(36) Miao, Q. Q.; Wu, L. Q.; Cui, J. N.; Huang, M. D.; Ma, T. L. *Adv. Mater.* **2011**, *23*, 2764−2768.
(37) Jeong, N. C.; Farha, O. K.; Hupp, J. T. *Langmuir* **2011**, *27*, 1996−1999.